Food Chemistry: X 15 (2022) 100436

Contents lists available at ScienceDirect

Food Chemistry: X

journal homepage: www.sciencedirect.com/journal/food-chemistry-x

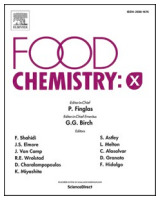

Waste Utilization: Physicochemical characteristics, stability and applications of emulsified *Rana chensinensis* ovum oil with waste extracts

Yongsheng Wang [a], Nan Li [a], Yuanshuai Gan [a], Changli Zhang [a], Shihan Wang [b], Zhongyao Wang [a], Zhihan Wang [a,*]

[a] School of Pharmaceutical Sciences, Jilin University, Changchun, Jilin 130021, China
[b] College of Chinese Medicinal Materials, Jilin Agricultural University, Changchun, Jilin 130118, China

ARTICLE INFO

Keywords:
Rana chensinensis ovum oil
Waste utilization
Protein isolate
Physicochemical characteristic
Quercetin

ABSTRACT

Rana chensinensis ovum (RCO) is the major waste/by-product of *Oviductus Ranae*. This study investigated physicochemical characteristics and stability of emulsified *Rana chensinensis* ovum oil (RCOO) with *Rana chensinensis* ovum protein isolates (RCOPI) by particle size, zeta potential, scanning electron microscopy (SEM), visual appearance, confocal laser scanning microscopy (CLSM), rheology and antioxidant capacity. The emulsified RCOO demonstrated great stability, antioxidant capacity and rheological properties. The potential application of the emulsified RCOO as a delivery system was studied using quercetin as an example. The stability of encapsulated quercetin was investigated through storage stability, thermal stability and photostability. The bioaccessibility of encapsulated quercetin was explored by *in vitro* digestion simulation experiments. The results showed the stability and bioaccessibility of quercetin encapsulated in emulsified RCOO was greatly improved. This study showed that the emulsified RCOO is a promising edible delivery system for hydrophobic bio-actives.

Introduction

In the food industry, large amounts of waste and by-product will be generated during the manufacture of final products (Ravindran & Jaiswal, 2016). Their generation and disposal are an emerging critical issue worldwide. Recent attention on food waste valorization has drawn great interest from industry and academia. Meanwhile, those industrial food waste and by-product are becoming a unique bioeconomic resource that can be processed to produce value-added products (Matharu, de Melo, & Houghton, 2016). This not only reduces waste and by-product disposal, but also regenerates resources from waste and by-product. The rational reuse of waste/by-product and the valorization of different components in waste/by-product can realize the sustainable industrialization of waste, bring high added value to them, and transform them from economic burden to economic success (Matharu et al., 2016). Moreover, the recovery of valuable components from waste and by-product as raw materials for future chemical, material and energy needs has greatly improved the utilization rate of waste/by-product, and is conducive to the creation of renewable supply chains to achieve a recycling economy (Xu, Nasrollahzadeh, Selva, Issaabadi, & Luque, 2019). The rational development and utilization of waste generated by the food industry as raw materials and re-purposed for nutrition and health purposes will be an important driving force for the future development of the food industry and will contribute to a more environmentally friendly and sustainable society (Ben-Othman, Jõudu, & Bhat, 2020).

Rana chensinensis ovum (RCO) is the main waste/by-product during the process of a traditional Chinese medicine and food, *Oviductus Ranae* (OR) (Liu et al., 2018). A large amount of RCO is discarded every year (Liu et al., 2018). In fact, RCO is the basis for the *Rana temporaria chensinensis* David to breed new life, and its nutritional value is very high. In addition, RCO can be cooked into delicious food, just like fish roe (Zhang et al., 2019). *Rana chensinensis* ovum oil (RCOO) is an extract of RCO using supercritical CO_2 fluid extraction technology, and has received approval from the China Food and Drug Administration as a functional food ("Rana chensinensis ovum soft capsule"). Previous research showed that RCOO is rich in unsaturated fatty acids such as eicosapentaenoic acid (EPA), α-Linolenic acid (ALA), docosahexaenoic acid (DHA), arachidonic acid (ARA), docosapentaenoic acid (DPA), linoleic acid (LA), oleic acid (OA), etc. (Gan et al., 2020). It was reported that RCOO can benefit human health, and has significant physiological functions in the prevention and treatment of cardiovascular diseases

* Corresponding author.
E-mail address: jluwang@jlu.edu.cn (Z. Wang).

https://doi.org/10.1016/j.fochx.2022.100436
Received 12 June 2022; Received in revised form 14 August 2022; Accepted 19 August 2022
Available online 23 August 2022
2590-1575/© 2022 The Author(s). Published by Elsevier Ltd. This is an open access article under the CC BY-NC-ND license (http://creativecommons.org/licenses/by-nc-nd/4.0/).

such as hyperlipidemia and thrombosis (Liu et al., 2018). However, RCOO is susceptible to oxidative rancidity, which limits its application in food industry. On the other hand, our previous study showed that the protein isolates recovered from *Rana chensinensis* ovum has great potential as a cheap and sustainable protein source in food applications (Li et al., 2022; Zhang et al., 2022). *Rana chensinensis* ovum protein isolates (RCOPI) not only have high nutrition, but also show outstanding functional properties such as water retention, oil retention, foaming ability, inhibition of linoleic acid oxidation and other aspects, making it a potential emulsified food protectant (Li et al., 2022; Zhang et al., 2022).

This work aimed to develop value-added products using RCOO and RCOPI that isolated from waste/by-product RCO. The physicochemical characteristics and stability of emulsified RCOO were studied by particle size, zeta potential, microstructure, stability, rheology, and antioxidant capacity. Furthermore, to explore the potential applications of emulsified RCOO as an edible delivery system, quercetin was encapsulated into the emulsified RCOO. Quercetin is a dietary flavonoid which shows great anticancer activity in various malignant tumors and plays an important role in preventing chronic diseases and promoting human health (Azeem et al., 2022). Although quercetin has variety physiological activities, its low solubility, stability, and bioavailability limit its physiological functions and applications. The stability and bioaccessibility of the encapsulated quercetin were investigated through storage stability, thermal stability, photostability and *in vitro* digestion experiments. This study is the first attempt to investigate the emulsified RCOO which will provide essential information for its further study.

Materials and methods

Materials

Raw *Rana chensinensis* ovum (RCO) was purchased from the main breeding area of Changbai Mountain (Jilin, China). CO_2 gas (99.5 %) was purchased from ZhongSheng Gas Co., Ltd. (Changchun, China). GDL (D-glucono-δ-lactone) was purchased from Yuanye Biochemical Reagent Co., Ltd. (Shanghai, China). Nile blue A, trichloroacetic acid and 1,1,3,3-tetraethoxypropane were purchased from Aladdin Biochemical Co., Ltd (Shanghai, China). Unless otherwise specified, other reagents were analytically pure and purchased from Macklin Biochemical Co., Ltd. (Shanghai, China).

Preparation of RCOO and RCOPI

The RCOO was extracted following the industrial process (Gan et al., 2020; Xu, Sun, & Xu, 2005). RCO powder was filtered with 40 mesh into the extraction kettle for supercritical CO_2 fluid extraction technology (CO_2-SFE) (Huaan Supercritical Extraction Corporation, China). CO_2 was used as the extraction solvent. The pressure of the extraction kettle was controlled at 35 MPa, at the temperature 29 °C for 180 min. Finally, the products extracted by supercritical fluid were collected from the separation kettle, weighed, and stored at –20 °C for further analysis.

The RCOO waste was dispersed in ultrapure water at the ratio of 1:15 (w/v) to form a uniform dispersion. 2 mol/L NaOH was used to adjust the dispersion to pH 11.0 and stirred at room temperature for 2 h. After centrifugation at 7650 g relative centrifugal force (RCF) for 10 min at 4 °C (H2050R-1, Cence, China), the supernatants were collected, and the precipitates were extracted again with 10 times volume of ultrapure water. Then supernatants were adjusted to pH 4.5 with 2 mol/L HCl and stored at 4 °C for 12 h to fully precipitate the dissolved protein. After centrifugation for 10 min (at 7650 g RCF, 4 °C), the protein precipitates were recovered and resuspended in a small amount of ultrapure water, and then adjusted to pH 7.0 with 2 mol/L NaOH to form protein concentrate. The protein concentrate was prefrozen at –20 °C for 12 h to form a stable solid, then the frozen samples were lyophilized at –80 °C for 48 h using a freeze dryer (Freezone 4.5L, Labconco Corporation, USA).

Preparation of RCOPI particles (RCOPPs)

The RCOPI (1.0 g) was mixed with 100 mL ultrapure water and the pH was adjusted to 12.5 with 2 mol/L NaOH. The mixture was stirred for 30 min until it was completely dissolved. Subsequently, hydrochloride (HCl, 2 mol/L), D-glucono-δ-lactone (GDL, 20 %) and critic acid (CA, 10 %) were added to the protein solution, respectively. The pH was adjusted to 7.5 to form RCOPI particles (RCOPPs, RCOPPs-HCl, RCOPPs-GDL, and RCOPPs-CA). The protein precipitates were stirred for 2 h until no visible particles were detected. The protein precipitates were recovered by centrifuge centrifugation at 7650 g RCF at 4 °C for 10 min. Samples were stored at 4 °C for further use.

Characterization of RCOPPs

Particle size and zeta potential

Particle size distribution and zeta potential of RCOPPs were determined using a combined dynamic light scattering/electrophoresis instrument (Zetasizer Nano-ZS, Malvern Instruments, UK). To avoid multiple particle effects, the RCOPPs dispersion was diluted 10 times with deionized water. All measurements were conducted at 25 °C.

Scanning electron microscope (SEM)

SEM (JSM-7900F, JEOL, Japan) was used to characterize the microstructure of RCOPPs. Prior to the observation, the surfaces of samples were sputtered and sprayed with gold to avoid charging under the electron beam. The typical SEM images of different samples were recorded under high vacuum with an accelerating voltage of 5 kV, and the magnifications of the observed samples were 20000 and 50000 times.

Fabrication of emulsified RCOO-RCOPPs

At a fixed oil–water ratio of 50 % and 2 mL of suspension, the RCOPPs-CA concentrations of 0.1 %, 0.25 %, 0.5 %, 1.0 %, 2.0 % and 4.0 % were homogenized with 2 mL of RCOO at 20000 rpm for 4 min (HR-500D, HUXI Corporation, China). At the fixed RCOPPs-CA concentration of 2.0 %, the RCOPPs-CA suspension was mixed with RCOO of 30 %, 40 %, 50 %, 60 %, 70 % and 80 % at 20000 rpm for 4 min.

Stabilization of emulsified RCOO-RCOPPs

Droplet size and zeta potential

The microstructure of emulsified RCOO-RCOPPs was observed with an optical microscope at 200 times magnification (BK6000, OPTEC, China). Image J was used to measure the droplet size and analyze the average emulsion droplet size based on randomly selected at least 600 emulsion droplets in different captured microscopic images. Measurements of zeta potential were carried out using an electrophoresis instrument (Zetasizer Nano-ZS, Malvern Instruments, U.K.). Before measurements, the samples were diluted 100 times with ultrapure water and loaded into disposable capillary cells (DTS1070).

Microstructure analysis

The morphology of emulsified RCOO-RCOPPs was observed by magnifying 200 times by optical microscope. The fresh emulsions were placed on the slides of the microscope. To avoid aggregation, the emulsions were diluted 2 times with 1.0 % SDS. The interfacial structure of the emulsions was observed by confocal laser scanning microscopy (CLSM, Leica TCS-SP8 STED, German). Before the observation, 0.1 mg/mL Nile red and 0.1 mg/mL Nile blue A mixture were used to dye the emulsions. The dyed samples were placed on the glass slide of the grooved laser confocal microscope, in which 488 nm was the excitation wavelength of Nile red and 633 nm was the excitation wavelength of Nile blue A.

Creaming index (CI)

Creaming is an index to show the separation process in which droplets flocculation and coalescence due to buoyancy movement, and can be measured by visual observation (Ju et al., 2020). The freshly prepared emulsified RCOO-RCOPPs were placed in glass vials. CI was observed and measured by vision, and then calculated according to equation (1).

$$CI = \frac{Hs}{He} \times 100\% \quad (1)$$

Hs represents the height of the water phase, and He represents the total height of the emulsion.

Rheological measurements

The rheological properties of emulsified RCOO-RCOPPs were studied by rheometer (ARES-G2, TA Instruments, USA). Appropriate amount of sample was placed on the flat plate to record the change of viscosity of the emulsion in the process of increasing the shear rate from 0.1 to 100 s^{-1}. Frequency scanning: under 1.0 % constant strain, the frequency increased from 0.1 to 100 rad/s, and the storage modulus (G') and loss modulus (G″) were recorded to characterize the dynamic viscoelasticity of emulsified RCOO-RCOPPs.

Lipid hydroperoxides (LH)

As the marker of the primary products of lipid oxidation, LH was determined according to the reported method with some modifications (Huang et al., 2019). Emulsified RCOO-RCOPPs (0.3 mL) were mixed with 1.5 mL of a 2-propanol and isooctane (1:3, v/v) solvent mixture and vortexed for 2 min, and then the mixture was centrifuged (4000 g RCF, 5 min). The organic phase (0.2 mL) was added to 2.8 mL of a methanol and 1-butanol mixture (2:1, v/v), followed by adding 50 μL of 3.94 mol/L NH_4SCN solution and 50 μL of Fe^{2+} solution, which was produced by mixing a 0.132 mol/L $BaCl_2$ solution with 0.144 mol/L $FeSO_4$. After 20 min of dark reaction at room temperature, the absorbance of the obtained solutions was measured at 510 nm, and the PV value in the emulsion can be calculated according to equation (2) (Li, Jiang, Zhang, Mu, & Liu, 2008).

$$PV(meq/kg) = \frac{A \times K \times 0.5}{55.86 \times m \times 2} \times 1000 \quad (2)$$

PV represents the peroxide value (meq/kg) in the sample. A represents the absorbance of the sample. K represents the slope of the Fe^{3+} calibration curve. 0.5 represents the molar ratio of O/Fe. 55.86 represents the atomic weight of Fe. The division by factor 2 is essential to express the peroxide value as milliequivalents of peroxide instead of milliequivalents of oxygen (Shantha & Decker, 1994).

Determination of malondialdehyde (MDA)

The content of MDA during storage was measured using the reported method (Ju et al., 2020). The sample (0.1 g) was dispersed in 1.9 mL of distilled water and 4.0 mL of solution was added (dissolved 15 g trichloroacetic acid (TCA) and 0.375 g thiobarbituric acid (TBA) in 100 mL of 0.25 mol/L HCl). The resultant mixtures were heated in a boiling water bath for 15 min and then cooled in the air to room temperature for approximately 10 min. After cooling down, supernatants were recovered by centrifugation at 11360 g RCF for 5 min, and the absorbance was measured at a wavelength of 532 nm. MDA concentration was determined according to calibration curve of 1,1,3,3-tetraethoxypropane.

Quercetin encapsulation (RCOO-RCOPPs-Q)

Preparation procedure

Quercetin was added to RCOO (0.15 mg/g) and stirred at 30 °C for 1 h. The RCOPPs-CA (2 mL) was mixed with RCOO (2 mL) in the glass bottle with the ratio of 1 to 1, and the RCOO-RCOPPs-Q was prepared by homogenizing at 20000 rpm for 4 min using a homogenizer equipped with the 8 mm diameter cutter head.

Encapsulation efficiency (EE)

The determination of quercetin in emulsions was conducted according to the reported approach (Wei et al., 2022). A mixed solvent (absolute ethanol/*n*-hexane = 2:3) was used to extract the quercetin encapsulated in samples. 1 mL of ethanol and *n*-hexane (2:3 v/v) was added to 200 μL of the sample. The extract was centrifuged at 4000 g (RCF) for 10 min to precipitate protein. Supernatants (800 μL) were added in a cuvette with 200 μL ethanol and *n*-hexane (2:3 v/v) to make a total volume of 1 mL. The absorbance of quercetin was recorded at 370 nm using a spectrophotometer (Sathishkumar et al., 2021). The quercetin concentration was then determined from a calibration curve prepared by dissolving known quantities of quercetin and calculated the encapsulation efficiency according to equation (3) (Wei et al., 2022).

$$EE\ (\%) = \frac{\text{encapsulated quercetin}}{\text{total quercetin}} \times 100 \quad (3)$$

Encapsulated quercetin represents the amount of quercetin in the emulsion, and total quercetin represents the amount of total quercetin added.

Storage stability

To study the storage stability of quercetin, RCOO-RCOPPs-Q and bulk oil loaded with quercetin were stored at 40 °C for 7 days. Three random samples were collected daily to determine quercetin retention. The samples were extracted with a mixture of 2 mL of ethanol and 3 mL of *n*-hexane, and centrifuged. The absorbance of the samples was then measured at 370 nm using a spectrophotometer. The quercetin concentration was then determined by the prepared calibration curve. The retention rate was calculated according to equation (4) (Huang et al., 2021).

$$\text{Retention}\ (\%) = \frac{C_t}{C_0} \times 100 \quad (4)$$

C_t represents the quercetin concentration after a period of storage, C_0 represents the initial quercetin concentration.

Thermal stability

RCOO-RCOPPs-Q and bulk oil loaded with quercetin were held for 6 h at 80 °C in dark. Three samples were collected randomly for the determination of quercetin retention at the interval of half hour.

Photostability

RCOO-RCOPPs-Q and bulk oil loaded with quercetin were irradiated under UV light for 5 h (4 w, 365 nm). Three samples were randomly collected every half hour to determine the retention of quercetin within 5 h intervals.

Free fatty acid (FFA) release and bioaccessibility

Simulated gastric fluid (SGF): SGF (1L) without pepsin was prepared by adding 2 g sodium chloride and then adjusting the pH to 1.5 by using 5 mol/L HCl. RCOO-RCOPPs or bulk oil containing 0.3 mg/g quercetin were mixed with 14 mL of SGF and stirred for 10 min at 37 °C. Then 3.2 mg pepsin was dissolved in 1 mL of SGF and then it was added to the previous mixture to start the digestion process. The obtained mixture was incubated for 2 h at 37 °C with shaking to simulate the gastric digestion process.

Simulated intestinal fluid (SIF): The pH of 30 mL of digested RCOO-RCOPPs-Q was adjusted to 7 to inactivate pepsin and terminate gastric digestion. Then 3.5 mL simulated intestinal fluid enzyme suspension (60 mg trypsin and 60 mg lipase in PBS, pH 7.0), salt solution (1.5 mL: 36.7 mg/mL $CaCl_2{\cdot}2H_2O$ and 218.7 mg/mL NaCl) and bile salt solution (2.5 mL:187.5 mg bile salt in PBS, pH 7.0) were added to the sample. The

pH of the mixed system was adjusted to 7.0, and 0.25 mol/L NaOH was added to maintain the pH during intestinal digestion. The simulated intestinal digestion was incubated for 2 h. The degree of lipolysis of the samples is expressed by the release of FFA. The volume of NaOH (0.25 mol/L) added over time was recorded to calculate the concentration of free fatty acids (FFA) produced by lipolysis according to equation (5) (Wei et al., 2022).

$$FFA(\%) = \frac{V_{NaOH} \times c_{NaOH} \times M_{lipid}}{W_{lipid} \times 2} \times 100 \quad (5)$$

V_{NaOH} (L) is the volume of sodium hydroxide required to neutralize the FFA produced, c_{NaOH} (mol/L) is the molarity of the sodium hydroxide solution used, W_{lipid} (g) is the total mass of RCOO initially present in the digestion, and M_{lipid} (g/mol) is the molecular mass of the triacylglycerol oil.

The original digesta was centrifuged at 13600 g (RCF) for 30 min and the middle micelle phase containing quercetin was collected. The bioaccessibility of quercetin was calculated using the following equation as described (Huang et al., 2021; Wei et al., 2022).

$$\text{Bioaccessibility}(\%) = \frac{C_{aqueous}}{C_{initial}} \times 100 \quad (6)$$

$C_{aqueous}$ represents the amount of quercetin left after digestion, $C_{initial}$ represents the original amount of quercetin encapsulated in the emulsions.

Statistical analysis

The experimental data of three parallel determinations was reported in the form of mean ± standard deviation. The data were analyzed using Origin 9.0 following *t*-test and one-way analysis of variance (ANOVA) by post hoc LSD test. Significant difference was defined as $p < 0.05$.

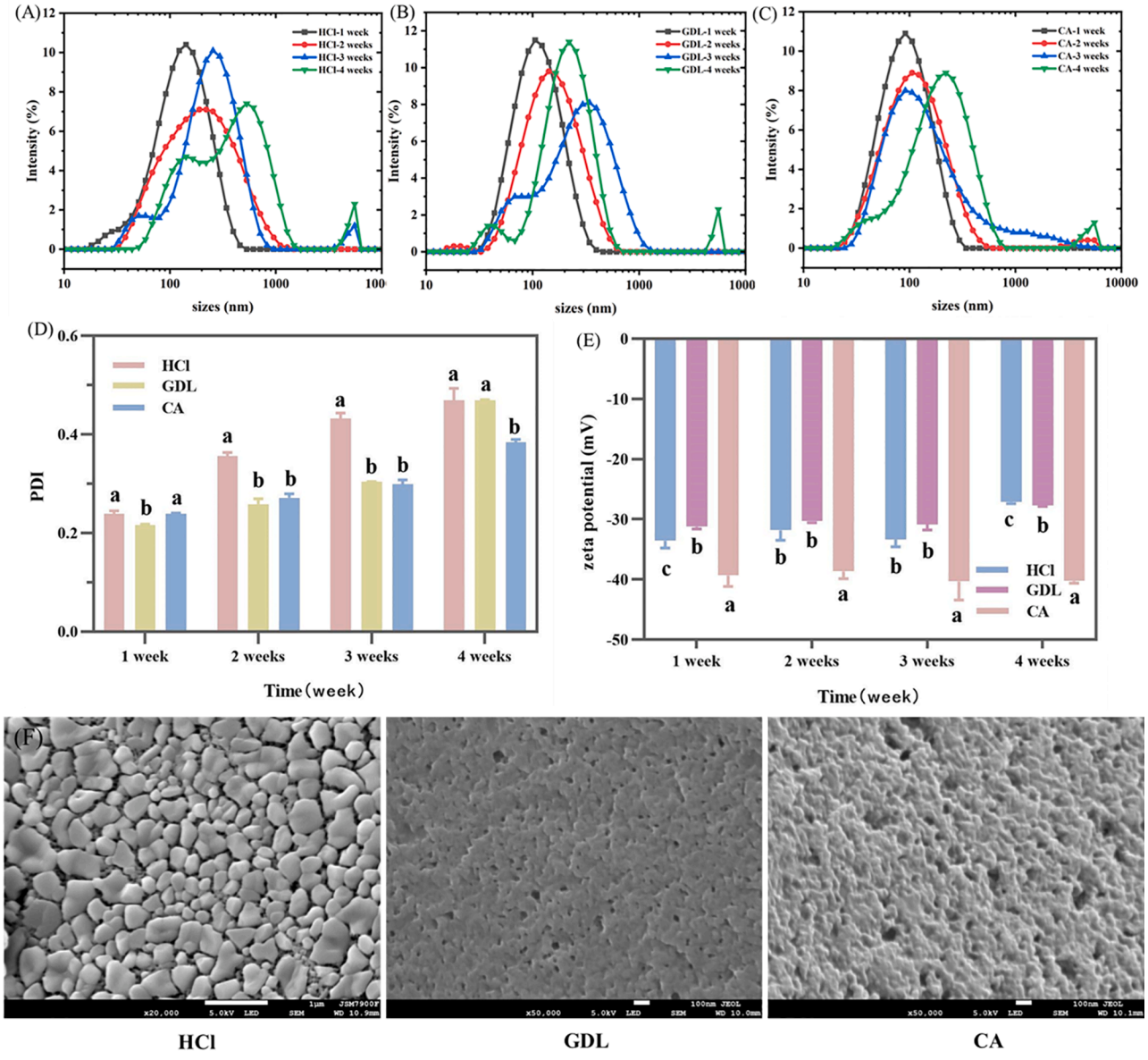

Fig. 1. Size distributions of pH 7.5 dispersions prepared with the pH cycling method using HCl (A), GDL (B) and CA (C), after storage at 4 °C for 4 weeks. Poly dispersibility index (PDI) (D) and zeta potential (E) of pH 7.5 dispersions prepared with the pH cycling method using HCl, GDL and CA, after storage at 4 °C for 4 weeks. SEM images of RCOPPs with the pH cycling method using HCl, GDL and CA (F). The scale bar is 200 nm in HCl, 100 nm in GDL and CA. (HCl, Hydrochloric acid; GDL, D-Glucono-δ-Lactone; CA, Citric acid). Different letters indicate significantly different values ($p < 0.05$).

Results and discussion

Investigation of RCOPI

Preparation of RCOO and RCOPI

RCOO was extracted from RCO using supercritical fluid extraction technology according to industrial operating procedures (Gan et al., 2020; Xu et al., 2005). The average yield of five times extraction was about 13 %. The waste residues were rich in proteins, accounting for more than 50 %, which was much higher than most typical high protein foods such as poultry (25 %), fish (20 %), and eggs (15 %). An alkali-solution and acid-isolation method was applied to extract the proteins in those waste (Gan et al., 2020; Li et al., 2022). The average isolation yield of RCOPI was 27 %. Pervious work showed that the RCOPI contains a complete range of amino acids and the essential amino acids required for human nutrition. The proportion of essential amino acids in the total amino acids is much higher than the recommended value of FAO (36 %) (FAO/WHO/UNU, 1985). Meanwhile, the content of sulfur-containing amino acids in RCOPI is more than 3.34 g/100 g, which is much higher than that of most plant proteins (Li et al., 2022). RCOPI is expected to be an ideal source of sulfur-containing amino acids, compared with many plant proteins.

Preparation and characterization of RCOPPs

The preparation of RCOPPs was based on the pH cycling method. When the pH of the RCOPI solution was gradually adjusted from 12.5 to 7.5, the sharp decrease in the solubility of RCOPI led to the self-assembly into relatively uniform colloidal particles. The particle size distribution of RCOPPs prepared with different acidifiers before and after storage for 4 weeks is shown in Fig. 1A, 1B and 1C. It was evident that the distribution of nanoparticles prepared by HCl, D-glucono-δ-lactone (GDL) and critic acid (CA) was unimodal. The average particle size of RCOPPs-CA was centered at 99 nm which was much smaller than that of RCOPPs-HCl and RCOPPs-GDL. After 4 weeks of storage, the particles prepared by HCl and GDL exhibited a significantly broader bimodal distribution, and the intensity (<100 nm) of the particles was <27 %, indicating that the RCOPPs aggregated and precipitated. However, the intensity (<100 nm) of particles prepared with CA was greater than 27 %, showing a smaller particle size. PDI represents droplet size distribution, low PDI represents uniform size distribution. The PDI of RCOPPs-HCl, RCOPPs-GDL and RCOPPs-CA was about 0.2, indicating those RCOPPs were homogeneous colloidal systems (Fig. 1D). The above results indicated RCOPPs-CA possess better anti-aggregation and precipitation stability than those prepared with HCl or GDL. This may be attributed to the denser structure of RCOPPs-CA, which reduced the contact with solvent water, thereby reducing the irregular motion of the colloidal system.

The sufficient surface electric charge of protein particles is one of the key factors to maintain the dispersion stability. Aggregation and conformational changes of protein particles can alter the surface charge properties, affecting the measured zeta potential. As shown in Fig. 1E, the zeta potential of RCOPPs-HCl and RCOPPs-GDL was about −30 mV and the zeta potential of RCOPPs-CA was about −40 mV, indicating that those colloid systems had sufficient electrostatic repulsion, and they can stably resist particle aggregation and stabilize the emulsions. Similar zeta potential properties were observed in RCOPPs-HCl and RCOPPs-GDL, indicating that the conformations of HCl and GDL were similar when the pH was lowered to a certain value. After 4 weeks of storage, the zeta potential of the RCOPPs did not change showing the great stability of those particles. RCOPPs-CA carried more electric charge and showed better stability than others.

SEM of RCOPPs

The morphology of the prepared RCOPPs was mainly spherical and elliptical (Fig. 1F), with weak aggregation of the particles. As shown in the SEM images, the morphology of the protein particles prepared after pH cycling with GDL and CA was different from that of HCl. Compared with the latter one, the former two RCOPPs exhibited more spherical, smaller, and more uniform particles. This difference may be caused by the distribution of hydroniums during the acidification process. The acidic process of GDL and CA treated samples was slow, resulting in small particle size and uniform particles, while HCl treated samples formed large particle size particles and led to precipitation. In addition, RCOPPs-GDL and RCOPPs-CA formed a compact network structure, which can provide more space for the capture of oil droplets. Overall, the SEM results were consistent with the dimension data, showing that the RCOPPs-CA were smaller and more uniform than RCOPPs-HCl and RCOPPs-GDL. The small size of particles mean that they had different physical, chemical and physiological characteristics from larger particles. This characteristic enabled them to be used in the production and development of various industries, such as pharmaceuticals, cosmetics and food industries (Tai et al., 2020).

Investigation of emulsified RCOO-RCOPPs

Effect of RCOPPs concentration

Fig. 2 shows the effect of different RCOPPs-CA concentrations on the size range and zeta potential of RCOO-RCOPPs emulsions when the fixed oil phase volume was 50 %. Optical microscopy is commonly used to detect flocculation, especially for droplets larger than 1 μm, and the microstructure of large particles can be evaluated based on morphology. Optical micrographs showed that the emulsion droplet structures of different concentrations of RCOPPs-CA were intact in structure without droplet collapse or droplet coalescence (Fig. 2A). As the RCOPPs-CA concentration increased from 0.1 % to 4.0 %, the droplet size continued to decrease (Fig. 2A and 2B). The observations suggested that with the initially formed oil–water interface and fixed particle migration rate, the more RCOPPs-CA anchored at the interface and the increased interfacial coverage as the concentration of particles in the aqueous phase increases. This contributes to the stabilization of the interfacial area in finite coalescence, a process known as “finite agglomeration”(Xu, Liu, & Tang, 2019).

When the solid particles exhibit weak adsorption at the interface, the particle surface charge is a factor affecting the stability of the emulsion. As the concentrations of RCOPPs-CA increased from 0.1 % to 4.0 %, the absolute value of the zeta potential increased from 30 mV to 47 mV (Fig. 2C). The increase of the negative surface charge enhanced the electrostatic repulsion between protein particles, which may effectively inhibit flocculation of the emulsion. This further interpreted that the RCOO stabilized by a high concentration of RCOPPs-CA had better stability. As previously reported, emulsions with zeta potential above 30 mV can be stabilized by electrostatic repulsion, similar to particle-stabilized emulsions such as zein/sodium caseinate (zein/ Nacas) (Wang & Zhang, 2017) and zein/chitosan (Liu, Chang, Shan, Fu, & Ding, 2021).

Effect of RCOO volume fraction

The RCOO volume fraction affects the droplets size and changes the type of emulsion obtained. When the RCOPPs-CA concentration was fixed at 2.0 %, the effect of RCOO volume fraction on the stability of RCOPPs-CA is shown in Fig. 3. As the proportion of RCOO increased from 30 % to 80 %, the changing trend of the emulsion droplet size was consistent with the microstructural observations in Fig. 3A and Fig. 3B. During the emulsification process, as the oil–water volume ratio increased, the small droplets in the emulsion aggregated into large droplets. This may be because it changed the number of particles that can be absorbed at the oil–water interface. As the oil volume fraction gradually increased from 30 % to 80 %, the higher the oil volume fraction, the larger the oil–water interface area, so the droplet size gradually became larger. This phenomenon can be understood that at a given concentration value, the amount of protein is usually insufficient to completely cover the interface of the new oil droplets generated during the emulsification process. The result is the formation of larger

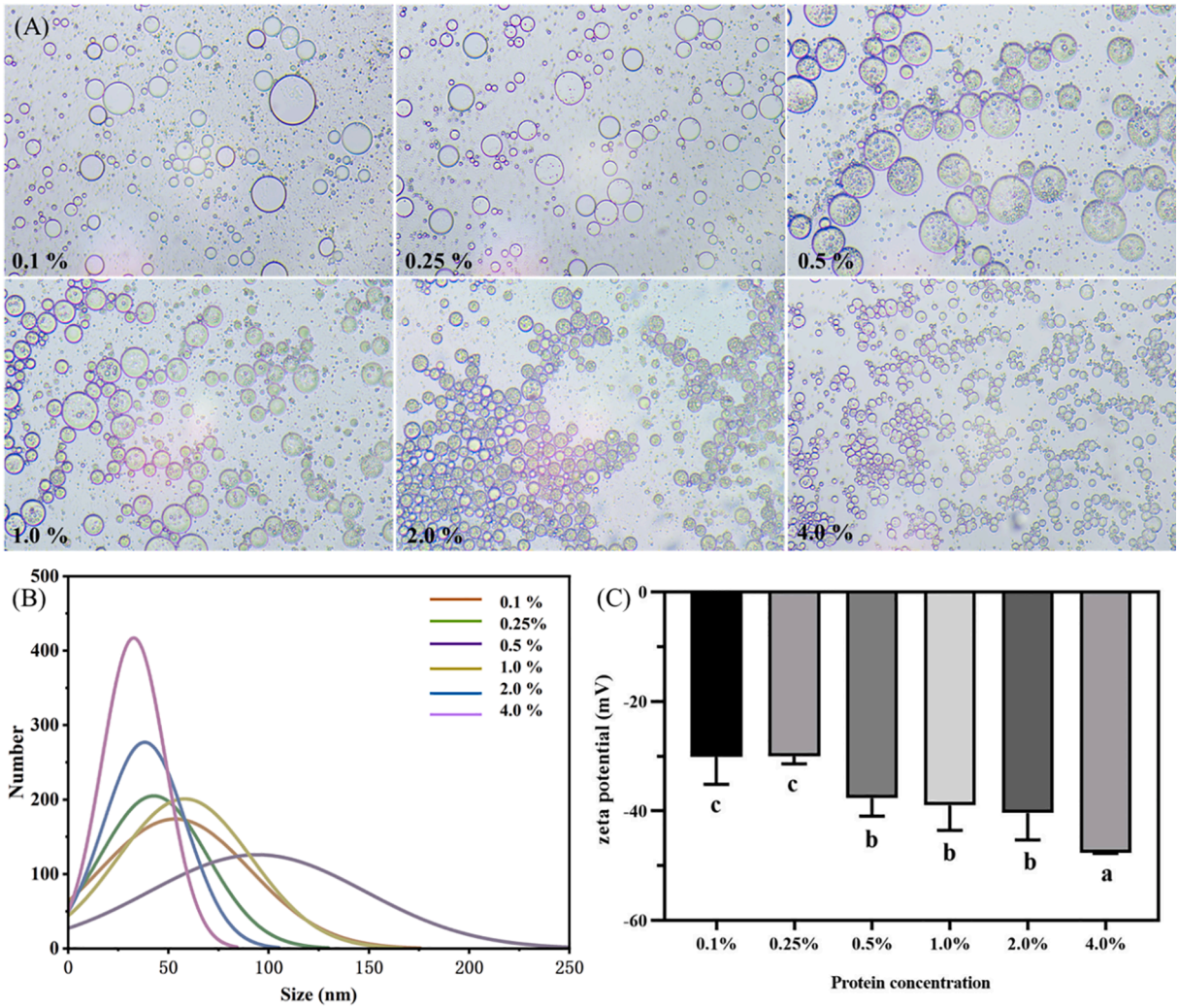

Fig. 2. Optical microscopy image with 200 × magnification (A) and droplet size distribution (B) and zeta potential (C) of the emulsified RCOO stabilized by RCOPPs-CA at different concentrations (0.1 %–4.0 %). Different letters indicate significantly different values ($p < 0.05$). (RCOPPs-CA: *Rana chensinensis* ovum protein isolates nanoparticles prepared by citric acid).

droplets and even droplet agglomeration and de-oiling. Similar results have also been reported in soybean protein particle aggregates (Liu & Tang, 2014). In addition, the zeta potential of emulsified RCOO-RCOPPs slightly changed as the oil–water ratio increased from 30 % to 80 % (Fig. 3C). The results indicated that the emulsified RCOO-RCOPPs had similar and high negative charges at different oil–water ratios. Such high zeta potential was expected to provide high repulsive forces between the droplets, inhibiting their coalescence and flocculation to stabilize the emulsion, which was consistent with the results of particle size analysis.

Confocal laser scanning microscopy (CLSM)

RCOO and RCOPPs-CA were stained with Nile Red (green) and Nile Blue A (red), respectively. Fig. 4 shows the distribution of RCOPPs-CA and RCOO in the emulsion. The green fluorescence channel represented RCOO, and the red fluorescence channel represented RCOPPs-CA (Fig. 4A and B). The yellow fluorescence channel was the result of the superposition of two substances (Fig. 4C), indicating that the emulsion had successfully integrated RCOPPs-CA and RCOO. The red fluorescence on the edges of the spherical droplets could be clearly observed under the fluorescence microscope. This phenomenon further indicated that O/W emulsions were prepared. In addition, the red fluorescent layer around the oil droplets was thin and dense, indicating that RCOPPs-CA adsorbed on the oil–water interface and formed a dense layer on the surface of spherical droplets (Fig. 4E and F). This property of RCOPPs is beneficial to improving stability of RCOO and reducing the risk of agglomeration and flocculation. Moreover, the use of RCOPPs as stabilizers instead of traditional hazardous surfactants can help reduce the toxicity of the formulation. It was reported that zein particles can stabilize oil droplets through a similar network structure formed on the droplets surface and in the surrounding aqueous phase (Zhu, Lu, Zhu, Zhang, & Yin, 2019). The above results suggested that RCOPPs-CA was ideal candidate for the protection of RCOO, which could act as stabilizers to adsorb at the O/W interface to form long-term stable O/W emulsions.

CI of RCOO-RCOPPs

Creaming is the physical instability caused by gravity separation, which reflects the storage stability of emulsions. It is an effective index to determine the separation degree of lipid and water phase in emulsions. The stability of emulsions stabilized by RCOPPs-CA was studied by the CI (understood as the relative ratio of water phase height to total height of emulsion). The smaller the CI, the better the stability of the emulsion.

The visual appearance and CI changes of different concentrations of RCOPPs-CA and different RCOO volume fractions after storage for 30 d are shown in Fig. 4G and H. With the increase of RCOPPs-CA concentrations, emulsified RCOO-RCOPPs gradually transitioned from a slightly stratified state to a non-stratified state with a significant increase

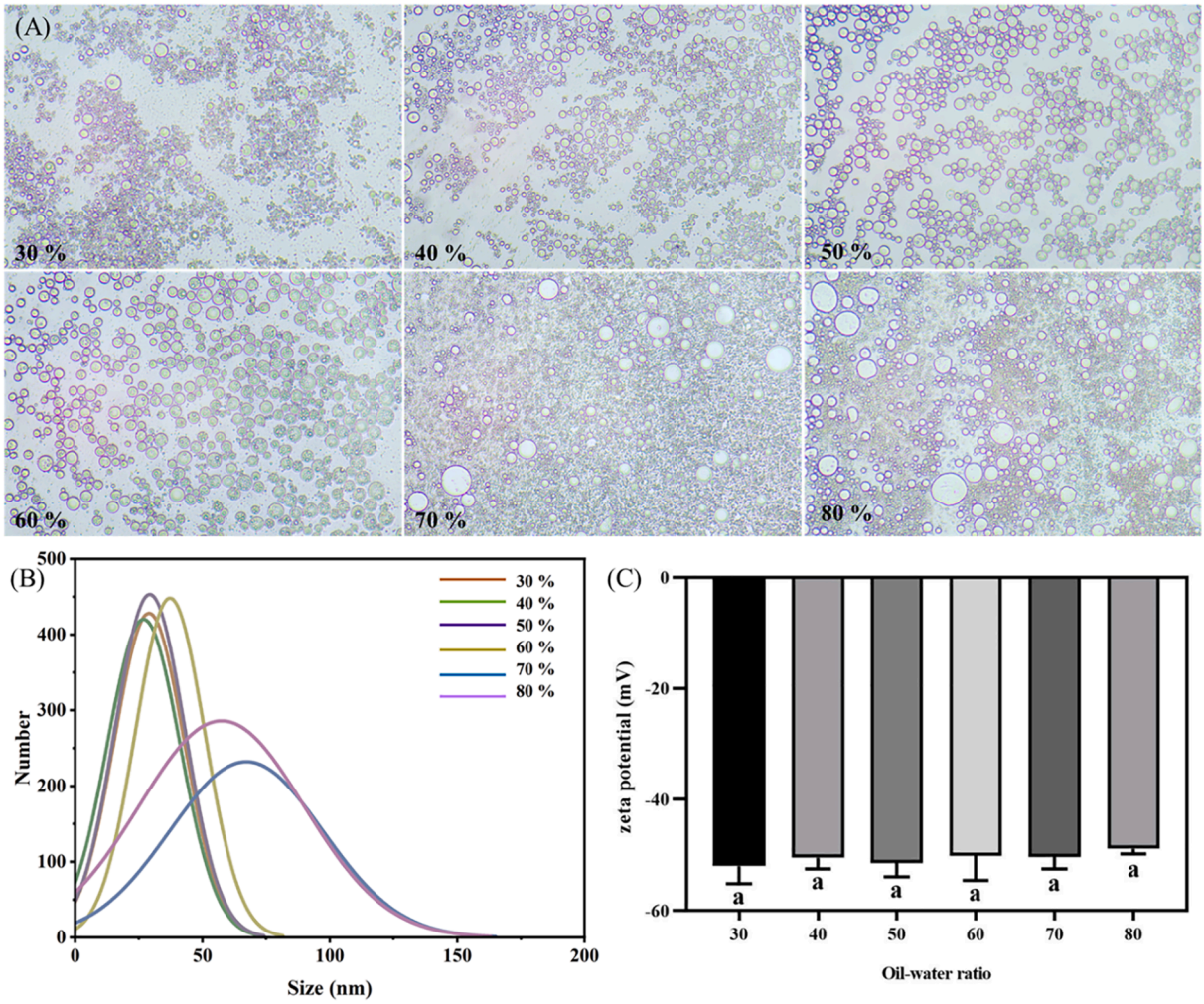

Fig. 3. Optical microscopy image with 200 × magnification (A) and droplet size distribution (B) and zeta potential (C) of the emulsified RCOO stabilized by RCOPPs-CA at different oil–water ratios (30 %–80 %). Different letters indicate significantly different values ($p < 0.05$). (RCOPPs-CA: *Rana chensinensis* ovum protein isolates nanoparticles prepared by citric acid).

in stability. This may be due to the further increase in viscosity with the increase of protein concentration, forming a gel-like network structure. The highly efficient and irreversible adsorption of high concentrations of protein particles at the oil–water interface acts as a unique physical barrier to protect oil droplets from coalescence and phase separation. Similar results in which the granule concentration affected the emulsion stability were also observed in chitosan particles (Li et al., 2019) and Gliadin (Zhou et al., 2018). In addition, the protein particles can improve the physical stability of RCOO-RCOPPs by reducing the interfacial free energy. During the homogenization process, small droplets formed by high concentrations of RCOPPs-CA were more resistant to gravitational separation and aggregation than larger droplets, thereby further stabilizing the emulsion. Within a certain range, the increase of the oil phase volume fraction led to an increase in the volume of the emulsified phase observed visually, and the CI gradually increased (Fig. 4I and J). When the oil volume fraction was low, the unstable water phase moved towards the bottom of the bottle due to gravity, and there were not enough droplets around to prevent it from moving, and delamination occurred. When the oil phase fraction was increased to 50 % and 60 %, there was no phase separation phenomenon, which could be explained by the aggregation effect (Zhang et al., 2021). Interestingly, with the further increase of the RCOO volume fraction, when the RCOO volume fraction reached 70 % and 80 %, the upper layer of the emulsion appeared oil-forming phenomenon. This may be due to the fact that the ratio of RCOPPs-CA was too small, and the oil–water interface was loosely arranged, which was not enough to cover the entire oil phase. At the same time, too many oil droplets in the emulsion tended to polymerize, resulting in instability of the emulsion and oil precipitation.

Rheological properties

Rheology is related to the stability, processing and application of emulsion (Jiang, Li, Du, Liu, & Meng, 2021). The rheological properties of emulsified RCOO-RCOPPs were characterized by steady flow method and dynamic oscillatory method. The apparent viscosity (η) of the emulsion decreased significantly when the shear rate was increased from 0.1 s to 100 s^{-1} (Fig. 5A and B), showing typical shear-thinning properties. This phenomenon can be attributed to the progressive deflocculation of oil droplets in the emulsion, where individual oil droplets or clusters of oil droplets were disrupted as the shear rate increases. Similar results were reported for Kafirin stabilized emulsions (Xiao, Wang, Perez Gonzalez, & Huang, 2016). The apparent viscosity increased with the increasing RCOPPs concentration from 0.1 % to 4.0 % (Fig. 5A), which may be due to the high bulk density of particles in the system and the formation of strong networks in the continuous phase. On the other hand, apparent viscosity increased with RCOO volume fraction in the range of 30 % to 60 %. When the volume fraction of RCOO increased to 70 % and 80 %, the apparent viscosity decreased dramatically. Due to the high-volume fraction of oil, the limited protein particles were not sufficient to stabilize all oil phases, resulting in a decrease in apparent viscosity. For dynamic oscillatory measurements,

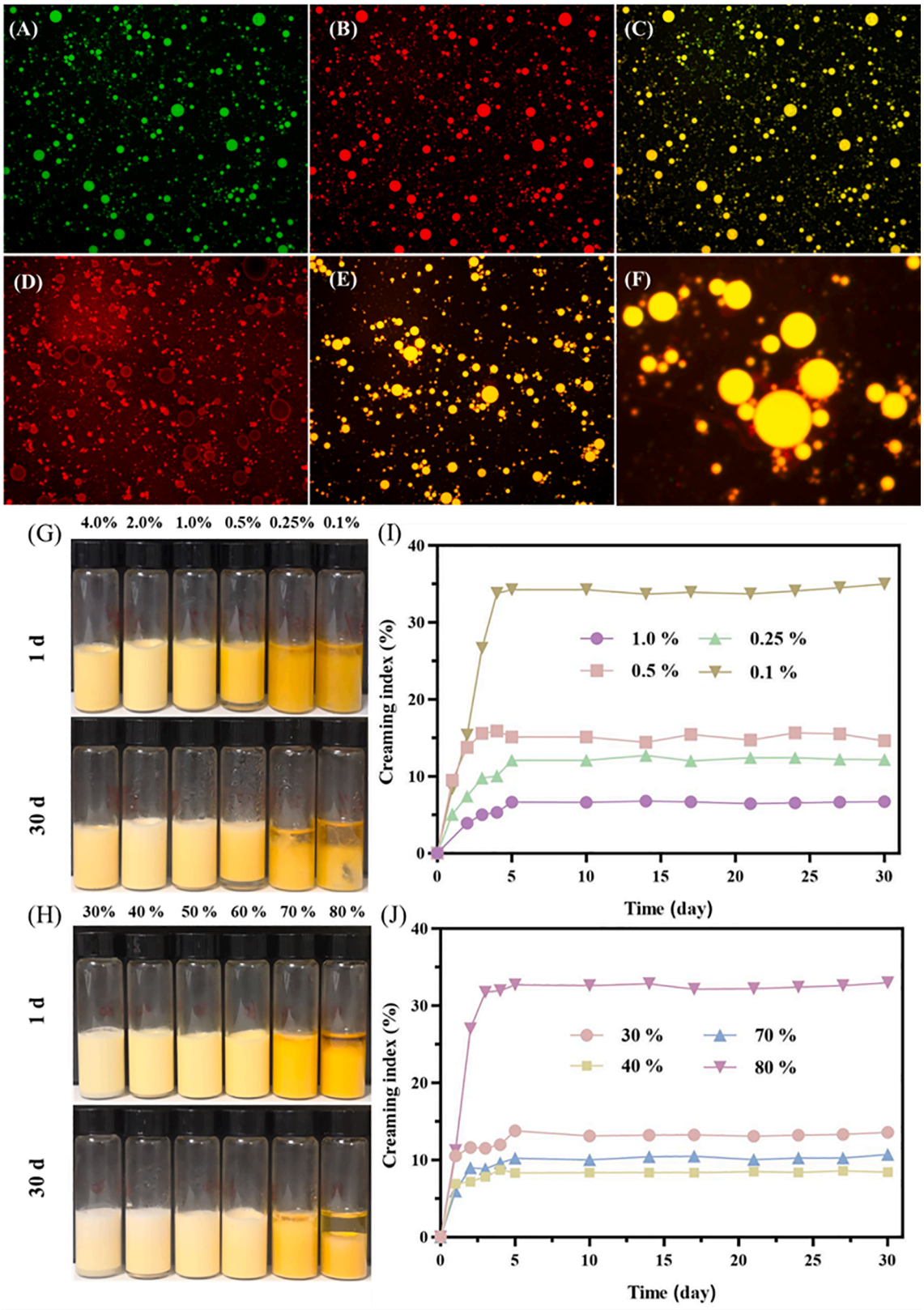

Fig. 4. CLSM images of emulsified RCOO stabilized by RCOPPs-CA with 2.0 % concentration and 50 % oil–water ratio. (A) *Rana chensinensis* ovum oil (RCOO) was stained by Nile Red excited at 488 nm (green). (B) RCOPPs-CA was stained by Nile Blue A excited at 633 nm (red). (C) was combined image of A and B. (D) was just stained by Nile Blue A excited at 633 nm. (E) and (F) shows the interface structure. Emulsified RCOO stabilized by RCOPPs-CA with different concentrations (0.1 %–4.0 %) and oil–water ratios (30 %–80 %). (G) and (H) are the visual appearance of emulsified RCOO stabilized by RCOPPs-CA after storage at room temperature for 1 d and 30 d. (I) and (J) are the changes of CI during storage of emulsion for 30 d.

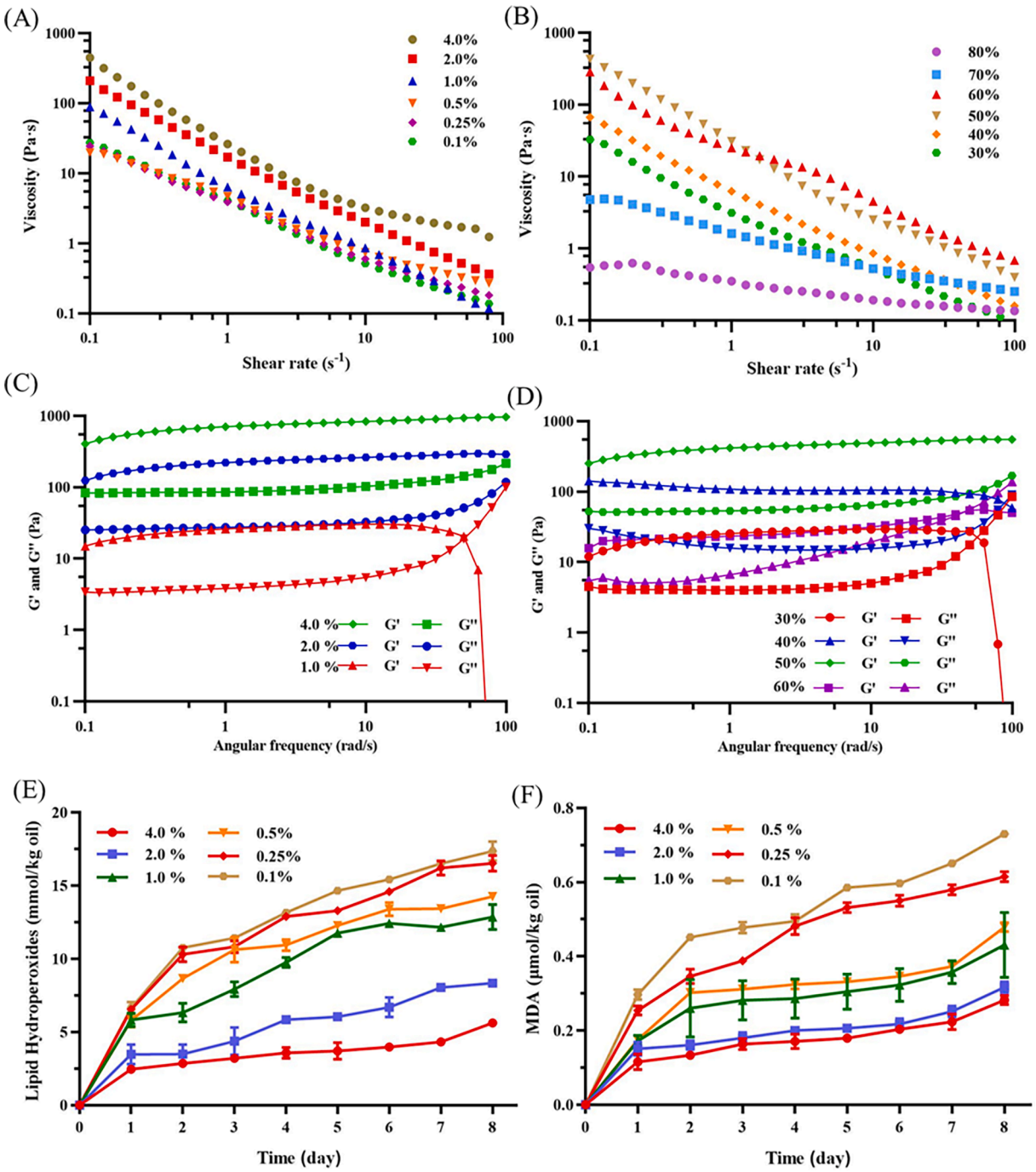

Fig. 5. (A) and (B) Apparent viscosity(η) of emulsified RCOO stabilized by RCOPPs-CA at different RCOPPs-CA concentrations (0.1 %–4.0 %) and oil–water ratios (30 %–80 %); (C) and (D) Storage modulus (G′) and loss modulus (G″) of emulsified RCOO stabilized by RCOPPs-CA at different concentrations (1.0 %–4.0 %) and oil–water ratios (30 %–60 %); Evolution of lipid hydroperoxides (LH) (E) and malondialdehyde (MDA) (F) prepared by different RCOPPs-CA concentrations (0.1 %–4.0 %) at 60 °C storage for up to 8 days. (RCOPPs-CA: *Rana chensinensis* ovum protein isolates nanoparticles prepared by citric acid).

the storage modulus (G') was always larger than the loss modulus (G") in the angular frequency range of 0.1 to 100 rad/s, indicating that the emulsion had an elastic gel structure. The two moduli were affected by the frequency, and it is a typical feature of highly flocculated elastic structures (Fig. 5C and D). The formation of this structure may be due to the formation of a thick particle layer at the oil–water interface and the 3D network of particles in the continuous phase.

Antioxidation properties

In this study, the initial degree of lipid oxidation and the development trend of oxidation reaction of RCOO-RCOPPs with different RCOPPs concentrations were evaluated using accelerated stability tests (Huang et al., 2019). Using peroxide value (PV) as the primary oxidation index and malondialdehyde (MDA) as the secondary oxidation index, the effects of different RCOPPs concentrations on the degree of oxidation were investigated. The tested MDA and lipid hydroperoxides (LH) content analysis results are shown in Fig. 5E and 5F. After 8 days of storage at 60 °C, the LH content of 0.1 % RCOPPs-CA changed from 6.63 ± 0.41 mmol/kg to 17.35 ± 0.65 mmol/kg and the MDA content changed from 0.29 ± 0.01 μmol/kg to 0.73 ± 0.04 μmol/kg. The LH content of 4.0 % RCOPPs-CA changed from 2.45 ± 0.24 mmol/kg to 5.62 ± 0.26 mmol/kg and the MDA content changed from 0.11 ± 0.02 μmol/kg to 0.28 ±

0.01 μmol/kg.

The above analysis showed the higher the RCOPPs concentration, the lower lipid peroxidation. RCOPPs can form tight interfacial layer on the surface of the RCOO droplets that acted as a physical barrier to prevent the transfer of oxidant and prevented the oil droplets being in close contact with oxidant in the continuous phase (Zhou et al., 2018). As shown in CLSM, RCOPPs formed a thick interfacial layer around the droplets, encapsulating the oil within it and maintaining the droplets integrity. As the concentration of RCOPPs increased, the free protein increased, exhibiting a higher system viscosity, thus forming a network in the continuous phase, and slowing down the movement of the oxidant (Zhu et al., 2019). In addition, RCOPPs carried negative charges and their side chains contained amino acids with antioxidant activity, such as methionine, cysteine, tryptophan, proline and histidine (Xiao, Li, & Huang, 2016), so the interfacial and free protein particles in the aqueous phase can scavenge free radicals and bind positively charged oxidants, further contributing to the reduction of lipid oxidation rate. This study showed the emulsified RCOO with RCOPPs is beneficial in delaying lipid

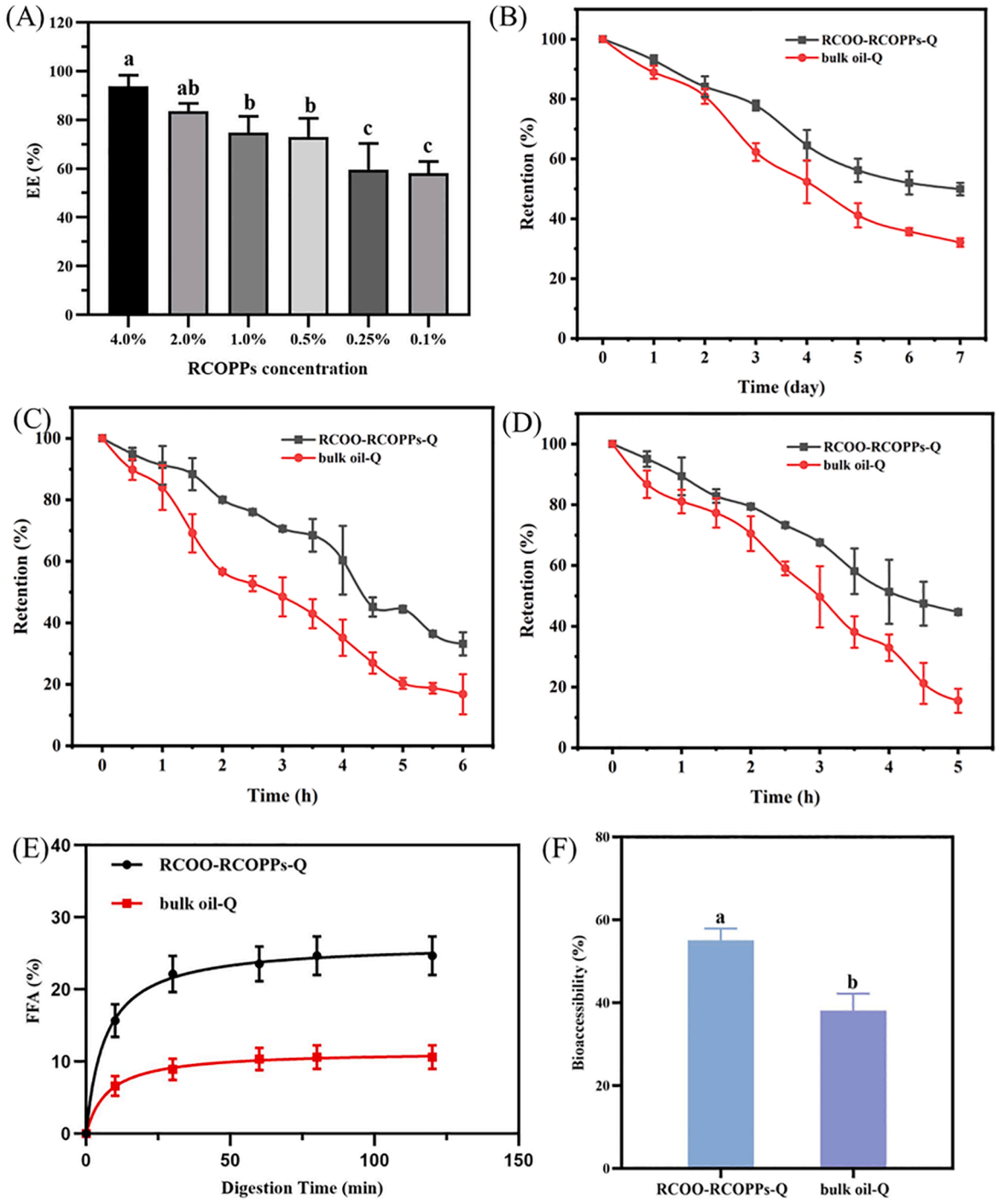

Fig. 6. (A) Encapsulation efficiency (EE) of quercetin in emulsified RCOO stabilized by RCOPPs-CA with different concentrations (0.1 %–4.0 %). Stability of quercetin protected by emulsified RCOO-RCOPPs and bulk oil (B) Storage stability (C) Thermal stability (D) Photostability. Different letters indicate significantly different values ($p < 0.05$). (E) Release profile of FFA in bulk oil and emulsified RCOO-RCOPPs. (F) Bioaccessibility of bulk oil and emulsified RCOO-RCOPPs. Different letters indicate significantly different values ($p < 0.05$). (RCOPPs-CA: *Rana chensinensis* ovum protein isolates nanoparticles prepared by citric acid).

oxidation.

Quercetin encapsulation (RCOO-RCOPPs-Q)

Encapsulation efficiency

Encapsulation has become an effective solution to improve the stability and bioavailability of hydrophobic bio-actives. In this study, the effect of different concentrations of RCOPPs on the encapsulation efficiency was investigated. RCOO stabilized by 0.1 % RCOPPs-CA showed the lowest EE among all samples (Fig. 6A) and the EE in RCOO increased to 93.76 ± 4.63 % when the RCOPPs-CA concentration increased to 4.0 %. The concentration of RCOPPs-CA showed an obvious positive correlation with the encapsulation efficiency, that was, the higher the concentration, the higher the EE. This phenomenon suggested that the interfacial composition was crucial for the viability of emulsified RCOO-RCOPPs as effective carriers of biologically active substances. Low concentrations of RCOPPs-CA were not sufficient to cover the droplet surface, resulting in the formation of an emulsion of large-sized droplets, which further led to the loss of bio-actives during the preparation of the emulsion. In addition, the low RCOPPs concentrations also led to more exposure of the RCOO located in the inner core to the external environment, resulting in the chemical degradation of quercetin under external stresses such as light, heat and oxygen.

Storage stability

To investigate the protective effect of emulsified RCOO-RCOPPs on quercetin, the retention of quercetin in RCOO-RCOPPs and bulk oil after being stored at 30 °C for 1 week was compared. As shown in Fig. 6B, the retention rates of quercetin encapsulated in emulsified RCOO-RCOPPs and bulk oil decreased to 49.92 ± 2.07 % and 32.10 ± 1.42 %, respectively after 1 week of storage. The results suggested that the quercetin-encapsulated emulsified RCOO-RCOPPs has superior stability. The dense packing of the particle not only made the emulsified RCOO-RCOPPs well stabilized through steric potential resistance and electrostatic repulsion, but also protected the interfacial layer containing bioactive components (Meng et al., 2020).

Thermal stability

Foods are usually heat-treated during the manufacturing process. Since quercetin is sensitive to heat treatment, the effect of heat treatment on the stability of quercetin in emulsified RCOO-RCOPPs and bulk oil loading was investigated. Fig. 6C shows the retention of quercetin in emulsified RCOO-RCOPPs and bulk oil after heating at 80 °C for 6 h. The quercetin content decreased significantly over time, especially in the first 4 h, which may be due to the isomerization and degradation of quercetin during heat treatment, as well as the acceleration of the oxidation process leading to quercetin structural changes in corticosteroids, thereby reducing retention (Han et al., 2021). After heat treatment for 6 h, the retention rates of quercetin in emulsified RCOO-RCOPPs and bulk oil decreased to 33.17 ± 2.66 % and 16.78 ± 4.62 %, respectively. The above results showed that quercetin in emulsified RCOO-RCOPPs was more stable to heat treatment. This might be because the RCOPPs-CA formed a physical barrier at the oil–water interface, which hindered the oxidative degradation of quercetin (Xiao, Li, & Huang, 2015).

Photostability

To investigate whether emulsified RCOO-RCOPPs has a protective effect on quercetin under UV irradiation, the retention rate of quercetin in emulsified RCOO-RCOPPs and bulk oil after UV irradiation for 5 h was studied (Fig. 6D). After UV irradiation for 5 h, the retention of quercetin in emulsified RCOO-RCOPPs and bulk oil decreased to 38.55 ± 0.03 % and 15.48 ± 0.04 %, respectively. In bulk oil, the quercetin molecules were directly exposed to UV radiation, while in emulsified RCOO-RCOPPs, the quercetin-rich dispersed phase in the aqueous phase was separated, leaving only the interfacial zone as a direct reaction zone for UV degradation. Compared to bulk oil, quercetin in emulsified RCOO-RCOPPs achieved better protection from direct UV radiation through the physical barrier of RCOPPs-CA. In addition, conjugated double bonds on tyrosine, phenylalanine, and tryptophan residues in RCOPI were able to absorb UV light, thereby protecting quercetin from degradation (Huang et al., 2021).

In vitro digestion of RCOO-RCOPPs-Q

The release of FFA

To investigate the application of emulsified RCOO-RCOPPs in the delivery of hydrophobic bio-actives, the *in vitro* digestion simulation experiments of stomach and intestine were performed. Fig. 6E shows that the digestion rate of RCOO-RCOPPs-Q was larger than that of the bulk oil. The RCOO-RCOPPs-Q showed a sharp release of FFA within 20 min after the start of digestion and reached a plateau after 60 min of digestion. The FFA release from bulk oil continued in a constant and slow manner until the end of digestion with RCOO-RCOPPs-Q (24.70 ± 2.66 %, 0.82 ± 0.08 mol/L) > bulk oil (10.60 ± 1.64 %, 0.35 ± 0.05 mol/L). The interfacial area of oil droplets in contact with lipase played an important role in determining the speed and extent of oil digestion (Liu & Tang, 2016). A larger interfacial area in contact with lipase can lead to a higher degree of lipolysis. The smaller droplet size exhibited by RCOO-RCOPPs-Q allowed for a larger interfacial area and therefore more accessible to lipases, facilitating faster lipolysis. In addition, in the process of gastrointestinal digestion, proteases such as pepsin and trypsin destroyed the structure of the interface by hydrolyzing RCOPPs-CA and made lipase and oil's direct contact possible, leading to the instability of emulsion. This facilitates faster lipolysis in RCOO-RCOPPs-Q. During gastrointestinal digestion, low pH also destabilized the structure of RCOO-RCOPPs-Q, causing the collapse of the interfacial layer of particles, which led to lipolysis. Overall, the FFA release rates (both < 50 %) indicated that the lipolysis efficiency of RCOO was not very high under the experimental conditions, which was consistent with the lipolysis efficiency of other long-chain oils (Xiao et al., 2015). Two factors are considered to be the main reasons for the inefficiency of lipolysis of long-chain oils. Long-chain fatty acids with poor water solubility were less accessible to contact and hydrolysis by pancreatic lipase in water system. Besides, the digestion products of long-chain oils were not easy to diffuse into the surrounding aqueous phase compared to short-chain oils, which further decreased the contact of lipase to the oil droplets (Liang et al., 2016).

Bioaccessibility

As shown in Fig. 6F, the bioaccessibility of RCOO-RCOPPs-Q (55.04 ± 2.3 %) was significantly higher than that in bulk oil (38.13 ± 3.3 %). The enhanced bioaccessibility was mainly due to the enhanced degree of lipid decomposition of the RCOO-RCOPPs. During lipid digestion, hydrolysis products such as diacylglycerols, monoglycerides and free fatty acids were released at the interface and formed micelles with bile salts and phospholipids, through which quercetin can be dissolved in the bulk oil, thus making quercetin bioaccessible (Zhang et al., 2021). As previously mentioned, more FFAs were released during the digestion of the protein particle-stabilized emulsion, which helped to generate more micelles to entrap quercetin, thereby improving the bioaccessibility of quercetin.

The results showed that the emulsified RCOO-RCOPPs had great stability and protective effect on hydrophobic bio-actives, demonstrating its potential application in drug delivery systems. The spatial physical barrier formed at the oil–water interface ensured the stability of certain photodegradable bioactive components. For the potential application of emulsified RCOO-RCOPPs in the food industry, more research is required in the following aspects in the future. It is necessary to investigate the degree of activity of the bioactive ingredients loaded in emulsified RCOO-RCOPPs during long-term storage or processing. The bioavailability of the encapsulated bioactive ingredients during *in*

vivo gastrointestinal digestion remains to be studied.

Conclusions

This study provided an effective strategy for realizing the value-added product using RCOO and RCOPI from by-product RCO. Accelerated stability and CLSM experiments showed that RCOPI can effectively improve the stability of emulsified RCOO. Emulsified RCOO-RCOPPs showed great performance, which gave them more possibilities for food applications. The bioactive substance delivery study of quercetin further demonstrated that emulsified RCOO-RCOPPs can protect quercetin from destruction and improve oral bioavailability, revealing the great potential of emulsified RCOO-RCOPPs in delivery. The results suggest that RCOO-RCOPPs is a promising delivery system, but further studies are required before their industrial application. For example, to demonstrate the delivery of bioactive substances by emulsified RCOO-RCOPPs, further studies on the decomposition of emulsified RCOO-RCOPPs in the human gastrointestinal tract and the effective release of nutrients are required in the future. Further research on how to improve the stability of emulsified RCOO-RCOPPs in food production and develop their commercial value in the food field can be conducted as well.

CRediT authorship contribution statement

Yongsheng Wang: Methodology, Validation, Formal analysis, Investigation, Data curation, Writing – original draft, Writing – review & editing, Visualization. **Nan Li:** Validation, Investigation, Writing – original draft, Writing – review & editing. **Yuanshuai Gan:** Formal analysis, Writing – original draft, Writing – review & editing. **Changli Zhang:** Investigation, Data curation, Writing – original draft. **Shihan Wang:** Investigation, Visualization, Writing – review & editing. **Zhongyao Wang:** Data curation, Writing – review & editing. **Zhihan Wang:** Methodology, Resources, Writing – review & editing, Supervision, Project administration, Funding acquisition.

Declaration of Competing Interest

The authors declare that they have no known competing financial interests or personal relationships that could have appeared to influence the work reported in this paper.

Acknowledgement

This work was supported by the Science and Technology Development Planning Project of Jilin Province [20200404037YY].

References

Azeem, M., Hanif, M., Mahmood, K., Ameer, N., Chughtai, F. R. S., & Abid, U. (2022). An insight into anticancer, antioxidant, antimicrobial, antidiabetic and anti-inflammatory effects of quercetin: A review. *Polymer Bulletin*.

Ben-Othman, S., Jõudu, I., & Bhat, R. (2020). Bioactives from Agri-Food Wastes: Present insights and future challenges. *Molecules, 25*(3).

FAO/WHO/UNU. (1985). Energy and protein requirements. Report of a joint FAO/WHO/UNU Expert Consultation. *World Health Organ Tech Rep Ser, 724*, 1-206.

Gan, Y., Xu, D., Zhang, J., Wang, Z., Wang, S., Guo, H., … Wang, Y. (2020). Rana chensinensis ovum oil based on CO_2 supercritical fluid extraction: response surface methodology optimization and unsaturated fatty acid ingredient analysis. *Molecules, 25*(18).

Han, L., Lu, K., Zhou, S., Zhang, S., Xie, F., Qi, B., & Li, Y. (2021). Development of an oil-in-water emulsion stabilized by a black bean protein-based nanocomplex for co-delivery of quercetin and perilla oil. *LWT, 138*, Article 110644.

Huang, M., Wang, Y., Ahmad, M., Ying, R., Wang, Y., & Tan, C. (2021). Fabrication of pickering high internal phase emulsions stabilized by pecan protein/xanthan gum for enhanced stability and bioaccessibility of quercetin. *Food Chemistry, 357*, Article 129732.

Huang, X., Zhou, F., Yang, T., Yin, S., Tang, C., & Yang, X. (2019). Fabrication and characterization of Pickering High Internal Phase Emulsions (HIPEs) stabilized by chitosan-caseinophosphopeptides nanocomplexes as oral delivery vehicles. *Food Hydrocolloids, 93*, 34–45.

Jiang, Q., Li, S., Du, L., Liu, Y., & Meng, Z. (2021). Soft κ-carrageenan microgels stabilized pickering emulsion gels: Compact interfacial layer construction and particle-dominated emulsion gelation. *Journal of Colloid and Interface Science, 602*, 822–833.

Ju, M., Zhu, G., Huang, G., Shen, X., Zhang, Y., Jiang, L., & Sui, X. (2020). A novel pickering emulsion produced using soy protein-anthocyanin complex nanoparticles. *Food Hydrocolloids, 99*, Article 105329.

Li, N., Wang, Y., Gan, Y., Wang, S., Wang, Z., Zhang, C., & Wang, Z. (2022). Physicochemical and functional properties of protein isolate recovered from Rana chensinensis ovum based on different drying techniques. *Food Chemistry, 396*, Article 133632.

Li, X., Xie, Q., Zhu, J., Pan, Y., Meng, R., Zhang, B., … Jin, Z. (2019). Chitosan hydrochloride/carboxymethyl starch complex nanogels as novel Pickering stabilizers: Physical stability and rheological properties. *Food Hydrocolloids, 93*, 215–225.

Li, Y., Jiang, B., Zhang, T., Mu, W., & Liu, J. (2008). Antioxidant and free radical-scavenging activities of chickpea protein hydrolysate (CPH). *Food Chemistry, 106*(2), 444–450.

Liang, R., Jiang, Y., Yokoyama, W., Yang, C., Cao, G., & Zhong, F. (2016). Preparation of Pickering emulsions with short, medium and long chain triacylglycerols stabilized by starch nanocrystals and their in vitro digestion properties. *RSC Advances, 6*(101), 99496–99508.

Liu, F., & Tang, C. (2014). Emulsifying properties of soy protein nanoparticles: Influence of the protein concentration and/or emulsification process. *Journal of Agricultural and Food Chemistry, 62*(12), 2644–2654.

Liu, F., & Tang, C. (2016). Soy glycinin as food-grade Pickering stabilizers: Part. III. Fabrication of gel-like emulsions and their potential as sustained-release delivery systems for β-carotene. *Food Hydrocolloids, 56*, 434–444.

Liu, J., Wu, S., Wang, D., Zhou, Q., Luo, Z., & Yu, H. (2018). Advances in research of the mutritional value and health function of ovum of Rana chensinensis. *Food Research and Development, 39*(11), 220–224.

Liu, Q., Chang, X., Shan, Y., Fu, F., & Ding, S. (2021). Fabrication and characterization of Pickering emulsion gels stabilized by zein/pullulan complex colloidal particles. *Journal of the Science of Food and Agriculture, 101*(9), 3630–3643.

Matharu, A. S., de Melo, E. M., & Houghton, J. A. (2016). Opportunity for high value-added chemicals from food supply chain wastes. *Bioresource Technology, 215*, 123–130.

Meng, R., Wu, Z., Xie, Q., Zhang, B., Li, X., Liu, W., … Li, P. (2020). Zein/carboxymethyl dextrin nanoparticles stabilized pickering emulsions as delivery vehicles: Effect of interfacial composition on lipid oxidation and in vitro digestion. *Food Hydrocolloids, 108*, Article 106020.

Rana chensinensis ovum soft capsule. Retrieved from: http://ypzsx.gsxt.gov.cn/specialfood/#/food Accessed Aug 11 2022.

Ravindran, R., & Jaiswal, A. K. (2016). Exploitation of food industry waste for high-value products. *Trends in Biotechnology, 34*(1), 58–69.

Sathishkumar, P., Li, Z., Govindan, R., Jayakumar, R., Wang, C., & Long, G. F. (2021). Zinc oxide-quercetin nanocomposite as a smart nano-drug delivery system: Molecular-level interaction studies. *Applied Surface Science, 536*, Article 147741.

Shantha, N. C., & Decker, E. A. (1994). Rapid, sensitive, iron-based spectrophotometric methods for determination of peroxide Values of food lipids. *Journal of AOAC International, 77*(2), 421–424.

Tai, Z., Huang, Y., Zhu, Q., Wu, W., Yi, T., Chen, Z., & Lu, Y. (2020). Utility of Pickering emulsions in improved oral drug delivery. *Drug Discovery Today, 25*(11), 2038–2045.

Wang, L., & Zhang, Y. (2017). Eugenol Nanoemulsion Stabilized with Zein and Sodium Caseinate by Self-Assembly. *Journal of Agricultural and Food Chemistry, 65*(14), 2990–2998.

Wei, Y., Wang, C., Liu, X., Mackie, A., Zhang, M., Dai, L., … Gao, Y. (2022). Co-encapsulation of curcumin and β-carotene in Pickering emulsions stabilized by complex nanoparticles: Effects of microfluidization and thermal treatment. *Food Hydrocolloids, 122*, Article 107064.

Xiao, J., Li, C., & Huang, Q. (2015). Kafirin nanoparticle-stabilized Pickering emulsions as oral delivery vehicles: physicochemical stability and in vitro digestion profile. *Journal of Agricultural and Food Chemistry, 63*(47), 10263–10270.

Xiao, J., Li, Y., & Huang, Q. (2016). Recent advances on food-grade particles stabilized Pickering emulsions: Fabrication, characterization and research trends. *Trends in Food Science & Technology, 55*, 48–60.

Xiao, J., Wang, X. A., Perez Gonzalez, A. J., & Huang, Q. (2016). Kafirin nanoparticles-stabilized Pickering emulsions: Microstructure and rheological behavior. *Food Hydrocolloids, 54*, 30–39.

Xu, C., Nasrollahzadeh, M., Selva, M., Issaabadi, Z., & Luque, R. (2019). Waste-to-wealth: Biowaste valorization into valuable bio(nano)materials. *Chemical Society Reviews, 48*(18), 4791–4822.

Xu, F., Sun, G., & Xu, J. Supercritical extraction process of Rana chensinensis ovum. CN1195049C, 2005-03-30, 2005.

Xu, Y., Liu, T., & Tang, C. (2019). Novel pickering high internal phase emulsion gels stabilized solely by soy β-conglycinin. *Food Hydrocolloids, 88*, 21–30.

Zhang, B., Meng, R., Li, X., Liu, W., Cheng, J., & Wang, W. (2021). Preparation of Pickering emulsion gels based on κ-carrageenan and covalent crosslinking with EDC: Gelation mechanism and bioaccessibility of curcumin. *Food Chemistry, 357*, Article 129726.

Zhang, T., Xu, J., Chen, J., Wang, Z., Wang, X., & Zhong, J. (2021). Protein nanoparticles for Pickering emulsions: A comprehensive review on their shapes, preparation methods, and modification methods. *Trends in Food Science & Technology, 113*, 26–41.

Zhang, Y., Wang, Y., Li, M., Liu, S., Yu, J., Yan, Z., & Zhou, H. (2019). Traditional uses, bioactive constituents, biological functions, and safety properties of *Oviductus ranae*

as functional foods in China. *Oxidative Medicine and Cellular Longevity, 2019*, 4739450.

Zhang, Y., Zhang, Y., Chen, N., Xin, N., Li, Q., Ye, H., … Zhang, T. (2022). Glycated modification of the protein from Rana chensinensis eggs by Millard reaction and its stability analysis in curcumin encapsulated emulsion system. *Food Chemistry, 382*, Article 132299.

Zhou, F., Huang, X., Wu, Z., Yin, S., Zhu, J., Tang, C., & Yang, X. (2018). Development of pickering emulsions stabilized by Gliadin/Proanthocyanidins Hybrid Particles (GPHPs) and the fate of lipid oxidation and digestion. *Journal of Agricultural and Food Chemistry, 66*(6), 1461–1471.

Zhu, Q., Lu, H., Zhu, J., Zhang, M., & Yin, L. (2019). Development and characterization of pickering emulsion stabilized by zein/corn fiber gum (CFG) complex colloidal particles. *Food Hydrocolloids, 91*, 204–213.